Group 4 Metal Olefin Polymerization Catalysts Stabilized by Bidentate O,P Ligands

Richard J. Long, Vernon C. Gibson,* and Andrew J. P. White

Department of Chemistry, Imperial College London, Exhibition Road, London, U.K., SW7 2AZ

Received August 9, 2007

A series of bis(phosphanylphenoxide) group 4 metal dichloride complexes has been synthesized via treatment of $MCl_4(THF)_2$ (M = Ti, Zr, Hf) with sodium salts of the phosphanylphenols. The complexes bearing diphenylphosphine donors adopt C_1-symmetric, all-*cis* ground-state structures as determined by X-ray crystallography. In solution an O,P ligand exchange process is observed. Eyring analyses indicate a nondissociative process proposed to proceed via a 120° rotation of the P,P,Cl or the O,P,Cl trigonal faces. A zirconium complex containing diisopropylphosphine donors adopts a configurationally rigid *trans*-P_2 geometry. In ethylene polymerization studies (methylaluminoxane (MAO) activation), bis(6-*tert*-butyl-2-diphenylphosphanylphenoxide) zirconium and hafnium catalysts gave activities up to 49 000 and 2000 g/mmol·h·bar, respectively. Both of these catalysts also afforded efficient catalyzed chain growth using $ZnEt_2$. The zirconium derivative afforded activities up to 13 300 g/mmol·h for propylene polymerization using "dried"-MAO (DMAO) as the cocatalyst. The polymer had a slight syndiotactic bias and is formed by a chain-end control mechanism. A dibenzyl analogue of the highly active zirconium catalyst revealed an all-*cis* structure by crystallography, but a mixture of isomers in solution by NMR spectroscopy. Cationic monoalkyl complexes were synthesized using either $[CPh_3][B(C_6F_5)_4]$ or DMAO and suggest a highly fluxional structure for the catalytically active species.

Introduction

Ligands containing monoanionic oxygen donors, especially phenoxides, have proved to be a popular alternative to the cyclopentadienyl fragment in post-metallocene olefin polymerization catalysts.[1] Although simple group 4 metal bis-phenoxide catalysts are active,[2] additional neutral donors are often incorporated into the ligand frame to occupy sites of coordinative unsaturation not needed for chain growth.[2a,b,3–19,21,22] Such additional donors may also help to "rigidify" the structure of the complex and open up the possibility for stereoselective polymerizations using prochiral olefins.

In group 4 metal complexes, the phenoxide donors tend to be matched with relatively hard first-row nitrogen-[3–18] and oxygen-based[7c,f−i,14c,h,19] donors. However, there is growing evidence that softer second-row donors may offer beneficial stabilization of the highly reactive metal center.[14c,h,20] While there have been a growing number of reports concerning catalysts that combine phenoxides with thioether donors[2a,b,7e,14c,h,19g,21,22] there has been little focus on ligands containing tertiary phosphines[14c,d,j,23,24] Therefore bis(*o*-phosphanylphenoxide) complexes of the group 4 metals[25,26] appeared attractive; additional benefits include (i) a fairly straightforward synthesis (*vide infra*) with several sites around the ligand amenable to elaboration, (ii) a rigid phenylene bridge, which should help to enforce phosphine coordination, and (iii) an active species that could

* To whom correspondence should be addressed. E-mail: v.gibson@imperial.ac.uk.

(1) (a) Britovsek, G. J. P.; Gibson, V. C.; Wass, D. F. *Angew. Chem., Int. Ed.* **1999**, *38*, 428. (b) Gibson, V. C.; Spitzmesser, S. K. *Chem. Rev.* **2003**, *103*, 283. (c) Suzuki, Y.; Terao, H.; Fujita, T. *Bull. Chem. Soc. Jpn.* **2003**, *76*, 1493. (d) Kawaguchi, H.; Matsuo, T. *J. Organomet. Chem.* **2004**, *689*, 4228.

(2) (a) van der Linden, A.; Schaverien, C. J.; Meijboom, N.; Ganter, C.; Orpen, A. G. *J. Am. Chem. Soc.* **1995**, *117*, 3008. (b) Sernetz, F. G.; Mülhaupt, R.; Fokken, S.; Okuda, J. *Macromolecules* **1997**, *30*, 1562. (c) Fokken, S.; Spaniol, T. P.; Okuda, J.; Sernetz, F. G.; Mülhaupt, R. *Organometallics* **1997**, *16*, 4240. (d) Thorn, M. G.; Etheridge, Z. C.; Fanwick, P. E.; Rothwell, I. P. *Organometallics* **1998**, *17*, 3636. (e) Thorn, M. G.; Etheridge, Z. C.; Fanwick, P. E.; Rothwell, I. P. *J. Organomet. Chem.* **1999**, *591*, 148.

(3) (a) For recent reviews on bis(phenoxyimine) catalysts see: Mitani, M.; Saito, J.; Ishii, S.-I.; Nakayama, Y.; Makio, H.; Matsukawa, N.; Matsui, S.; Mohri, J.-I.; Furuyama, R.; Terao, H.; Bando, H.; Tanaka, H.; Fujita, T. *Chem. Rec.* **2004**, *4*, 137. (b) Nakayama, Y.; Bando, H.; Sonobe, Y.; Fujita, T. *Bull. Chem. Soc. Jpn.* **2004**, *77*, 617. (c) Makio, H.; Fujita, T. *Bull. Chem. Soc. Jpn.* **2005**, *78*, 52. (d) Sakuma, A.; Weiser, M.-S.; Fujita, T. *Polym. J.* **2007**, *39*, 193.

(4) Suzuki, Y.; Kashiwa, N.; Fujita, T. *Chem. Lett.* **2002**, *358*.

(5) (a) Repo, T.; Klinga, M.; Pietikäinen, P.; Leskelä, M.; Uusitalo, A.-M.; Pakkanen, T.; Hakala, K.; Aaltonen, P.; Löfgren, B. *Macromolecules* **1997**, *30*, 171. (b) Huang, J.; Lian, B.; Yong, L.; Qian, Y. *Inorg. Chem. Commun.* **2001**, *4*, 392. (c) Knight, P. D.; Clarke, A. J.; Kimberley, B. S.; Jackson, R. A.; Scott, P. *Chem. Commun.* **2002**, *352*. (d) Ishii, S.; Mitani, M.; Saito, J.; Matsuura, S.; Furuyama, R.; Fujita, T. *Stud. Surf. Sci. Catal.* **2003**, *145*, 49. (e) Wang, M.; Zhu, H.; Jin, K.; Dai, D.; Sun, L. *J. Catal.* **2003**, *220*, 392. (f) Cuomo, C.; Strianese, M.; Cuenca, T.; Sanz, M.; Grassi, A. *Macromolecules* **2004**, *37*, 7469. (g) Zhu, H.; Wang, M.; Ma, C.; Li, B.; Chen, C.; Sun, L. *J. Organomet. Chem.* **2005**, *690*, 3929. (h) Lamberti, M.; Consolmagno, M.; Mazzeo, M.; Pellecchia, C. *Macromol. Rapid Commun.* **2005**, *26*, 1866. (i) Strianese, M.; Lamberti, M.; Mazzeo, M.; Tedesco, C.; Pellecchia, C. *J. Mol. Catal. A: Chem.* **2006**, *258*, 284. (j) Clarkson, G. J.; Gibson, V. C.; Goh, P. K. Y.; Hammond, M. L.; Knight, P. D.; Scott, P.; Smit, T. M.; White, A. J. P.; Williams, D. J. *Dalton Trans.* **2006**, *5484*.

(6) (a) Tshuva, E. Y.; Goldberg, I.; Kol, M. *J. Am. Chem. Soc.* **2000**, *122*, 10706. (b) Busico, V.; Cipullo, R.; Ronca, S.; Budzelaar, P. H. M. *Macromol. Rapid Commun.* **2001**, *22*, 1405. (c) Busico, V.; Cipullo, R.; Friederichs, N.; Ronca, S.; Togrou, M. *Macromolecules* **2003**, *36*, 3806. (d) Busico, V.; Cipullo, R.; Friederichs, N.; Ronca, S.; Talarico, G.; Togrou, M.; Wang, B. *Macromolecules* **2004**, *37*, 8201. (e) Segal, S.; Goldberg, I.; Kol, M. *Organometallics* **2005**, *24*, 200. (f) Yeori, A.; Goldberg, I.; Shuster, M.; Kol, M. *J. Am. Chem. Soc.* **2006**, *128*, 13062. (g) Busico, V.; Cipullo, R.; Pellecchia, R.; Ronca, S.; Roviello, G.; Talarico, G. *Proc. Natl. Acad. Sci. U.S.A.* **2006**, *103*, 15321.

10.1021/om7008149 CCC: $40.75
Publication on Web 12/29/2007

parallel the highly active group 4 metal phenoxyimine systems[3] and offer a new class of early transition metal polymerization catalyst with the potential to influence polymer microstructure and stereochemistry.

Results and Discussion

Complex Synthesis and Structure. A range of *ortho*-substituted phosphanylphenols was synthesized from the corresponding phenols using the MOM protection, lithiation, deprotection strategy of Rauchfuss[27] (Scheme 1). In each case a hitherto unreported phosphonium salt was obtained that required treatment with ammonia to effect deprotection of the proligand. This product (**A**) was isolated and characterized during the synthesis of 6-(*tert*-butyl)-2-diphenylphosphanylphenol and revealed a hydroxymethyl substituent attached to the phosphorus center, presumably formed by an intramolecular attack during the MOM deprotection (Scheme 2; the structure of the salt was confirmed by crystallography; see Supporting Information).

(7) (a) Tshuva, E. Y.; Goldberg, I.; Kol, M.; Goldschmidt, Z. *Inorg. Chem. Commun.* **2000**, *3*, 611. (b) Tshuva, E. Y.; Goldberg, I.; Kol, M.; Weitman, H.; Goldschmidt, Z. *Chem. Commun.* **2000**, *379*. (c) Tshuva, E. Y.; Goldberg, I.; Kol, M.; Goldschmidt, Z. *Chem. Commun.* **2001**, *2120*. (d) Tshuva, E. Y.; Goldberg, I.; Kol, M.; Goldschmidt, Z. *Organometallics* **2001**, *20*, 3017. (e) Groysman, S.; Tshuva, E. Y.; Reshef, D.; Gendler, S.; Goldberg, I.; Kol, M.; Goldschmidt, Z.; Shuster, M.; Lidor, G. *Isr. J. Chem.* **2002**, *42*, 373. (f) Tshuva, E. Y.; Groysman, S.; Goldberg, I.; Kol, M.; Goldschmidt, Z. *Organometallics* **2002**, *21*, 662. (g) Groysman, S.; Goldberg, I.; Kol, M.; Genizi, E.; Goldschmidt, Z. *Inorg. Chim. Acta* **2003**, *345*, 137. (h) Groysman, S.; Goldberg, I.; Kol, M.; Genizi, E.; Goldschmidt, Z. *Organometallics* **2003**, *22*, 3013. (i) Groysman, S.; Tshuva, E. Y.; Goldberg, I.; Kol, M.; Goldschmidt, Z.; Shuster, M. *Organometallics* **2004**, *23*, 5291. (j) Reybuck, S. E.; Lincoln, A. L.; Ma, S.; Waymouth, R. M. *Macromolecules* **2005**, *38*, 2552. (k) Gendler, S.; Groysman, S.; Goldschmidt, Z.; Shuster, M.; Kol, M. *J. Polym. Sci., Part A: Polym. Chem.* **2006**, *44*, 1136.

(8) (a) Huang, J.; Lian, B.; Qian, Y.; Zhou, W.; Chen, W.; Zheng, G. *Macromolecules* **2002**, *35*, 4871. (b) Bott, R. K. J.; Hughes, D. L.; Schormann, M.; Bochmann, M.; Lancaster, S. J. *J. Organomet. Chem.* **2003**, *665*, 135. (c) Sanz, M.; Cuenca, T.; Galakhov, M.; Grassi, A.; Bott, R. K. J.; Hughes, D. L.; Lancaster, S. J.; Bochmann, M. *Organometallics* **2004**, *23*, 5324. (d) Chen, Q.; Huang, J.; Yu, J. *Inorg. Chem. Commun.* **2005**, *8*, 444. (e) Coles, S. R.; Clarkson, G. J.; Gott, A. L.; Munslow, I. J.; Spitzmesser, S. K.; Scott, P. *Organometallics* **2006**, *25*, 6019.

(9) (a) Chan, M. C. W.; Tam, K.-H.; Pui, Y.-L.; Zhu, N. *J. Chem. Soc., Dalton Trans.* **2002**, *3085*. (b) Chan, M. C. W.; Tam, K.-H.; Zhu, N.; Chiu, P.; Matsui, S. *Organometallics* **2006**, *25*, 785.

(10) Kui, S. C. F.; Zhu, N.; Chan, M. C. W. *Angew. Chem., Int. Ed.* **2003**, *42*, 1628.

(11) Bei, X.; Swenson, D. C.; Jordan, R. F. *Organometallics* **1997**, *16*, 3282.

(12) Inoue, Y.; Nakano, T.; Tanaka, H.; Kashiwa, N.; Fujita, T. *Chem. Lett.* **2001**, *1060*.

(13) (a) Cozzi, P. G.; Gallo, E.; Floriani, C.; Chiesi-Villa, A.; Rizzoli, C. *Organometallics* **1995**, *14*, 4994. (b) Bott, R. K. J.; Hammond, M.; Horton, P. N.; Lancaster, S. J.; Bochmann, M.; Scott, P. *Dalton Trans.* **2005**, *3611*.

(14) (a) Pennington, D. A.; Hughes, D. L.; Bochmann, M.; Lancaster, S. J. *Dalton Trans.* **2003**, *3480*. (b) Owiny, D.; Parkin, S.; Ladipo, F. T. *J. Organomet. Chem.* **2003**, *678*, 134. (c) Oakes, D. C. H.; Kimberley, B. S.; Gibson, V. C.; Jones, D. J.; White, A. J. P.; Williams, D. J. *Chem. Commun.* **2004**, *2174*. (d) Hu, W.-Q.; Sun, X.-L.; Wang, C.; Gao, Y.; Tang, Y.; Shi, L.-P.; Xia, W.; Sun, J.; Dai, H.-L.; Li, X.-Q.; Yao, X.-L.; Wang, X.-R. *Organometallics* **2004**, *23*, 1684. (e) Pennington, D. A.; Clegg, W.; Coles, S. J.; Harrington, R. W.; Hursthouse, M. B.; Hughes, D. L.; Light, M. E.; Schormann, M.; Bochmann, M.; Lancaster, S. J. *Dalton Trans.* **2005**, *561*. (f) Wang, C.; Sun, X.-L.; Guo, Y.-H.; Gao, Y.; Liu, B.; Ma, Z.; Xia, W.; Shi, L.-P.; Tang, Y. *Macromol. Rapid Commun.* **2005**, *26*, 1609. (g) Oakes, D. C. H.; Gibson, V. C.; White, A. J. P.; Williams, D. J. *Inorg. Chem.* **2006**, *45*, 3476. (h) Wang, C.; Ma, Z.; Sun, X.-L.; Gao, Y.; Guo, Y.-H.; Tang, Y.; Shi, L.-P. *Organometallics* **2006**, *25*, 3259. (i) Paolucci, G.; Zanella, A.; Sperni, L.; Bertolasi, V.; Mazzeo, M.; Pellecchia, C. *J. Mol. Catal. A: Chem.* **2006**, *258*, 275. (j) Said, M.; Hughes, D. L.; Bochmann, M. *Inorg. Chim. Acta* **2006**, *359*, 3467.

(15) (a) Milione, S.; Montefusco, C.; Cuenca, T.; Grassi, A. *Chem. Commun.* **2003**, *1176*. (b) Milione, S.; Bertolasi, V.; Cuenca, T.; Grassi, A. *Organometallics* **2005**, *24*, 4915. (c) Cuomo, C.; Milione, S.; Grassi, A. *Macromol. Rapid Commun.* **2006**, *27*, 611.

(16) Kraft, B. M.; Huang, K.-W.; Cole, A. P.; Waymouth, R. M. *Helv. Chim. Acta* **2006**, *89*, 1589.

(17) (a) Wang, W.; Fujiki, M.; Nomura, K. *Macromol. Rapid Commun.* **2004**, *25*, 504. (b) Padmanabhan, S.; Katao, S.; Nomura, K. *Organometallics* **2007**, *26*, 1616.

(18) (a) Pennington, D. A.; Coles, S. J.; Hursthouse, M. B.; Bochmann, M.; Lancaster, S. J. *Chem. Commun.* **2005**, *3150*. (b) Pennington, D. A.; Coles, S. J.; Hursthouse, M. B.; Bochmann, M.; Lancaster, S. J. *Macromol. Rapid Commun.* **2006**, *27*, 599. (c) Bryliakov, K. P.; Kravtsov, E. A.; Broomfield, L.; Talsi, E. P.; Bochmann, M. *Organometallics* **2007**, *26*, 288.

(19) (a) Matilainen, L.; Klinga, M.; Leskelä, M. *J. Chem. Soc., Dalton Trans.* **1996**, *219*. (b) Sobota, P.; Przybylak, K.; Utko, J.; Jerzykiewicz, L. B.; Pombeiro, A. J. L.; Guedes da Silva, M. F. C.; Szczegot, K. *Chem.−Eur. J.* **2001**, *7*, 951. (c) Motta, O.; Capacchione, C.; Proto, A.; Acierno, D. *Polymer* **2002**, *43*, 5847. (d) Capacchione, C.; Neri, P.; Proto, A. *Inorg. Chem. Commun.* **2003**, *6*, 339. (e) Reimer, V.; Spaniol, T. P.; Okuda, J.; Ebeling, H.; Tuchbreiter, A.; Mulhaupt, R. *Inorg. Chim. Acta* **2003**, *345*, 221. (f) Suzuki, Y.; Inoue, Y.; Tanaka, H.; Fujita, T. *Macromol. Rapid Commun.* **2004**, *25*, 493. (g) Boussie, T. R.; Brümmer, O.; Diamond, G. M.; Goh, C.; LaPointe, A. M.; Leclerc, M. K.; Shoemaker, J. A. W. (Symyx Technologies, Inc.) US 7126031 B2, 2006.

(20) (a) Froese, R. D. J.; Musaev, D. G.; Matsubara, T.; Morokuma, K. *J. Am. Chem. Soc.* **1997**, *119*, 7190. (b) Froese, R. D. J.; Musaev, D. G.; Matsubara, T.; Morokuma, K. *Organometallics* **1999**, *18*, 373. (c) Porri, L.; Ripa, A.; Colombo, P.; Miano, E.; Capelli, S.; Meille, S. V. *J. Organomet. Chem.* **1996**, *514*, 213. (d) Lavanant, L.; Silvestru, A.; Faucheux, A.; Toupet, L.; Jordan, R. F.; Carpentier, J. F. *Organometallics* **2005**, *24*, 5604.

(21) (a) Miyatake, T.; Mizunuma, K.; Seki, Y.; Kakugo, M. *Makromol. Chem., Rapid Commun.* **1989**, *10*, 349. (b) Miyatake, T.; Mizunuma, K.; Kakugo, M. *Makromol. Chem., Macromol. Symp.* **1993**, *66*, 203. (c) Fokken, S.; Spaniol, T. P.; Kang, H. C.; Massa, W.; Okuda, J. *Organometallics* **1996**, *15*, 5069. (d) Janas, Z.; Jerzykiewicz, L. B.; Przybylak, K.; Sobota, P.; Szczegot, K. *Eur. J. Inorg. Chem.* **2004**, *1639*. (e) Natrajan, L. S.; Wilson, C.; Okuda, J.; Arnold, P. L. *Eur. J. Inorg. Chem.* **2004**, *3724*. (f) Janas, Z.; Jerzykiewicz, L. B.; Przybylak, K.; Sobota, P.; Szczegot, K.; Wisniewska, D. *Eur. J. Inorg. Chem.* **2005**, *1063*. (g) Janas, Z.; Jerzykiewicz, L. B.; Sobota, P.; Szczegot, K.; Wisniewska, D. *Organometallics* **2005**, *24*, 3987. (h) Wisniewska, D.; Janas, Z.; Sobota, P.; Jerzykiewicz, L. B. *Organometallics* **2006**, *25*, 6166.

(22) (a) Capacchione, C.; Proto, A.; Ebeling, H.; Muelhaupt, R.; Moller, K.; Spaniol, T. P.; Okuda, J. *J. Am. Chem. Soc.* **2003**, *125*, 4964. (b) Proto, A.; Capacchione, C.; Venditto, V.; Okuda, J. *Macromolecules* **2003**, *36*, 9249. (c) Capacchione, C.; Proto, A.; Ebeling, H.; Mulhaupt, R.; Moller, K.; Manivannan, R.; Spaniol, T. P.; Okuda, J. *J. Mol. Catal. A, Chem.* **2004**, *213*, 137. (d) Capacchione, C.; D'Acunzi, M.; Motta, O.; Oliva, L.; Proto, A.; Okuda, J. *Macromol. Chem. Phys.* **2004**, *205*, 370. (e) Capacchione, C.; Proto, A.; Okuda, J. *J. Polym. Sci., Part A: Polym. Chem.* **2004**, *42*, 2815. (f) Beckerle, K.; Capacchione, C.; Ebeling, H.; Manivannan, R.; Mulhaupt, R.; Proto, A.; Spaniol, T. P.; Okuda, J. *J. Organomet. Chem.* **2004**, *689*, 4636. (g) Capacchione, C.; De Carlo, F.; Zannoni, C.; Okuda, J.; Proto, A. *Macromolecules* **2004**, *37*, 8918. (h) Capacchione, C.; Manivannan, R.; Barone, M.; Beckerle, K.; Centore, R.; Oliva, L.; Proto, A.; Tuzi, A.; Spaniol, T. P.; Okuda, J. *Organometallics* **2005**, *24*, 2971. (i) De Carlo, F.; Capacchione, C.; Schiavo, V.; Proto, A. *J. Polym. Sci., Part A: Polym. Chem.* **2006**, *44*, 1486. (j) Capacchione, C.; Proto, A.; Ebeling, H.; Mülhaupt, R.; Okuda, J. *J. Polym. Sci., Part A: Polym. Chem.* **2006**, *44*, 1908. (k) Beckerle, K.; Manivannan, R.; Spaniol, H. P.; Okuda, J. *Organometallics* **2006**, *25*, 3019.

(23) (a) Baxter, S. M.; Wolczanski, P. T. O,P ligated group 4 metal complexes that have not been evaluated for olefin polymerization include the following. *Organometallics* **1990**, *9*, 2498. (b) van Doorn, J. A.; van der Heijden, H.; Orpen, A. G. *Organometallics* **1994**, *13*, 4271. (c) Miquel; L.; Bassobert, M.; Choukroun, R.; Madhouni, R.; Eichhorn, B.; Sanchez, M.; Mazières, M. R.; Jaud, J. *J. Organomet. Chem.* **1995**, *490*, 21. (d) Willoughby, C. A.; Duff, R. R.; Davis, W. M.; Buchwald, S. L. *Organometallics* **1996**, *15*, 472. (e) Priya, S.; Balakrishna, M. S.; Mague, J. T. *Chem. Lett.* **2004**, *33*, 308. (f) Liang, L.-C.; Chang, Y.-N.; Lee, H. M. *Inorg. Chem.* **2007**, *46*, 2666.

(24) O,P nickel complexes have been extensively studied as oligomerization catalysts. For a recent review see: Kuhn, P.; Sémeril, D.; Matt, D.; Chetcuti, M. J.; Lutz, P. *Dalton Trans.* **2007**, *515*.

(25) Long, R. J.; Gibson, V. C.; White, A. J. P.; Williams, D. J. *Inorg. Chem.* **2006**, *45*, 511.

(26) (a) Kashiwamura, T.; Okamoto, T. (Idemitsu Petrochemical Co.) US 6730626 B2, 2004. (b) Gibson, V. C.; Jacobsen, G. B.; Jones, D. J.; Long, R. J. (Innovene Europe Ltd) US 7144839 B2, 2006.

(27) Rauchfuss, T. B. *Inorg. Chem.* **1977**, *16*, 2966.

Scheme 1. Synthesis of Bis(phosphanylphenoxide)M(IV) Dichloride Complexes (OMOM = OCH_2OCH_3)

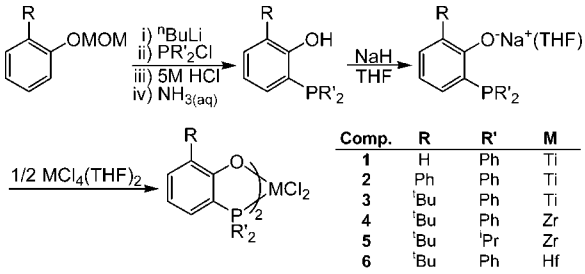

Comp.	R	R'	M
1	H	Ph	Ti
2	Ph	Ph	Ti
3	tBu	Ph	Ti
4	tBu	Ph	Zr
5	tBu	iPr	Zr
6	tBu	Ph	Hf

Scheme 2. Proposed Mechanism for Formation of A

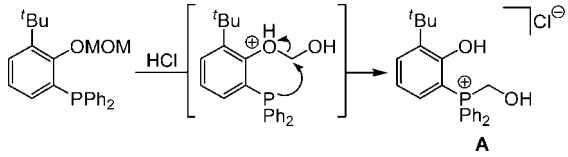

The phosphanylphenols were converted to sodium salts using NaH and reacted with $MCl_4(THF)_2$ (M = Ti, Zr, and Hf) to give the desired complexes **1**−**6** as analytically pure air- and moisture-sensitive solids (Scheme 1). The bis-O,P structures of **1** and **3**−**6** were confirmed by single-crystal X-ray analyses. The structures of **3** and **4** are discussed below; analyses of **1**, **5**, and **6** have been reported previously and revealed all-*cis* structures for **1** and **6** and a *trans*-P_2 structure for **5**.[25]

The solid-state structure of **3** revealed the presence of two crystallographically independent molecules (**I** and **II**) in the asymmetric unit (molecule **I** is shown in Figure 1, molecule **II** in Figure S4 in the Supporting Information). The coordination sphere for each molecule is distorted octahedral with *cis* angles being in the ranges 73.81(7)–105.87(7)° and 71.81(6)–101.22(7)° for molecules **I** and **II**, respectively; the two most acute angles in each case are associated with the bites of the O,P ligands. The primary difference between the molecules is not the arrangement of the donor atoms, which, like in **1** and **6**, are all-*cis*, but the conformation of the P(1)/O(1) ligand. This difference can be readily appreciated by considering the folding of the five-membered C_2OPTi chelate rings. While for both complexes the P(2)/O(2) ring is essentially planar (the five atoms being coplanar to within ca. 0.03 and 0.01 Å for molecules **I** and **II**, respectively), the P(1)/O(1) ring in each case has an envelope conformation with the metal lying out of the C_2OP plane (coplanar to within ca. 0.02 Å). For molecule **I** the metal lies ca. 0.57 Å out of this plane in the direction of O(2), whereas for molecule **II** the metal lies ca. 0.63 Å in the opposite direction toward Cl(2′). Keeping the Ti,Cl(1),Cl(2),P(2),O(1),O(2) coordination sphere "stationary" (these atoms have an rms fit of ca. 0.06 Å in the two molecules), this difference can be viewed as a bending of the aryl ring of the P(1)/O(1) ligand about the P···O vector either toward or away from O(2) (see Figure S6 in the Supporting Information). This flexing is accompanied by a shift in the P(1) position between the two molecules by ca. 0.37 Å. The different conformations of the C_2OPTi rings may be caused by steric interactions between the two *tert*-butyl substituents as the analogous chelates in **1** are planar to within 0.04 Å.[25] The *trans* influence of the various donors can be seen by inspection of the Ti−X bond lengths (Table 1). The Ti−P(1) bond is longer than its Ti−P(2) counterpart, reflecting the difference between a chloride and a (phen)oxide, respectively, in the *trans* position. Likewise, Ti−Cl(2) is longer than Ti−Cl(1), reflecting the difference between a formally monoanionic oxygen donor and a neutral phosphorus donor, and Ti−O(2) is longer than Ti−O(1) [in complex **I** but not, strangely, in complex **II**], showing the difference between chloride and phosphorus.

Table 1. Selected Bond Lengths (Å) and Angles (deg) for Complexes 3 (molecules I and II), 4, and 6

	3 (**I**) [M = Ti]	**3** (**II**) [M = Ti]	**4** [M = Zr]	**6** [M = Hf]
M−O(1)	1.839(2)	1.8388(19)	1.9632(15)	1.956(3)
M−O(2)	1.874(2)	1.837(2)	1.9889(14)	1.989(3)
M−P(1)	2.7055(8)	2.7408(9)	2.8872(6)	2.8628(11)
M−P(2)	2.6309(8)	2.6979(9)	2.8208(6)	2.7954(11)
M−Cl(1)	2.2679(9)	2.2794(9)	2.4239(6)	2.4058(11)
M−Cl(2)	2.3177(8)	2.3307(9)	2.4263(6)	2.4060(12)
Cl(1)−M−P(1)	178.98(4)	170.81(4)	170.66(2)	169.99(4)
Cl(2)−M−O(2)	161.34(7)	160.62(7)	154.08(5)	155.76(10)
P(2)−M−O(1)	159.34(7)	163.71(7)	152.95(5)	154.30(10)
Cl(1)−M−Cl(2)	94.95(3)	94.15(3)	96.87(2)	96.37(5)
Cl(1)−M−P(2)	92.18(3)	92.88(3)	103.30(2)	103.34(4)
Cl(1)−M−O(1)	105.87(7)	101.22(7)	101.81(5)	100.33(10)
Cl(1)−M−O(2)	93.52(7)	95.13(8)	92.55(5)	92.43(9)
Cl(2)−M−P(1)	86.07(3)	81.17(3)	85.026(19)	86.04(4)
Cl(2)−M−P(2)	88.05(3)	89.03(3)	84.69(2)	85.37(4)
Cl(2)−M−O(1)	100.04(7)	97.95(7)	102.16(5)	101.88(11)
P(1)−M−P(2)	87.96(2)	94.94(3)	85.965(16)	86.52(3)
P(1)−M−O(1)	73.81(7)	71.81(6)	68.86(5)	69.66(10)
P(1)−M−O(2)	85.54(6)	91.73(7)	89.57(4)	89.20(9)
P(2)−M−O(2)	75.03(6)	73.54(6)	69.62(4)	70.61(9)
O(1)−M−O(2)	93.57(9)	96.89(9)	99.44(6)	98.68(14)

The crystal structure of the zirconium complex **4** (Figure 2) is very similar to that of **3**-**I**. The geometry at the metal center is distorted octahedral with *cis* angles in the range 68.86(5)–103.30(2)°. The coordination sphere is all-*cis*, and the two five-membered C_2OPZr chelate rings have different geometries; the P(2)/O(2)

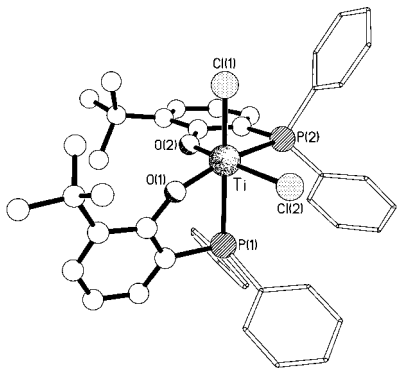

Figure 1. Molecular structure of **I**, one of the two independent molecules present in the crystals of **3**.

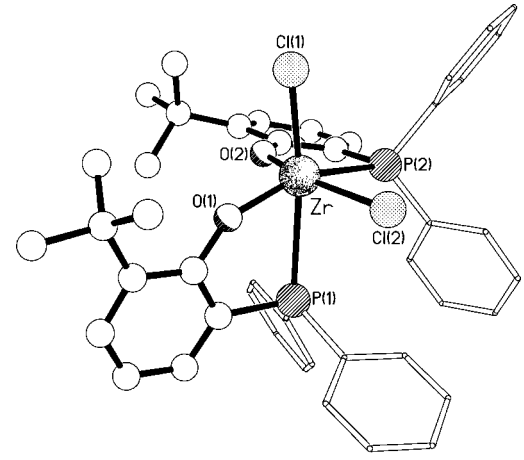

Figure 2. Molecular structure of **4**.

Scheme 3. Interchange of all-*cis* enantiomers.

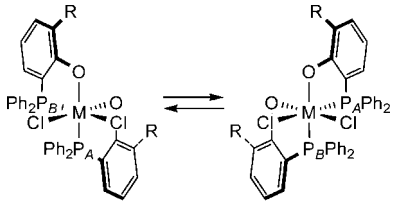

ring is flat (all five atoms coplanar to within ca. 0.03 Å), while the P(1)/O(1) ring has an envelope conformation with the metal lying ca. 0.36 Å out of the C_2OP plane (which is coplanar to within ca. 0.02 Å) in the direction of O(2).[28] This planarity for the P(2)/O(2) ring, and folding of the P(1)/O(1) ring, is also seen in the structure of the hafnium analogue **6**,[25] where the five atoms of the P(2)/O(2) ring are all coplanar to within ca. 0.03 Å, and the metal lies ca. 0.37 Å out of the $C_2O(1)P(1)$ plane (which is coplanar to within ca. 0.02 Å) in the direction of O(2).[29] The most noticeable difference between complexes **3** and **4** (except the obvious presence of only one independent molecule in the structure of **4**) is in the pattern of bonding at the metal center (Table 1). Although the bonds to phosphorus and oxygen show the same pattern as in **3** [M−P(1) longer than M−P(2), M−O(2) longer than M−O(1)], the two Zr−Cl bond lengths are statistically identical [2.4239(6) and 2.4263(6) Å to Cl(1) and Cl(2), respectively], whereas in **3** the Ti−Cl(2) bonds were noticeably longer than those to Cl(1). This may in part be a consequence of the Zr−Cl bonds being ca. 0.1 Å longer than their Ti−Cl counterparts. This pattern of bond lengths is repeated in the hafnium analogue **6** (Table 1).

The configurations of **1**−**6** in solution were determined by ^{1}H and ^{31}P NMR spectroscopy. All signals in the ^{31}P spectra were shifted substantially downfield (by 16–30 ppm) from the value found for the corresponding sodium phosphanylphenoxide, consistent with coordination of the phosphines to the metal center.[23b,d] If, as seen in the solid state, the PPh_2-substituted complexes adopt a C_1-symmetric, all-*cis* configuration, then two sets of signals are expected for the inequivalent O,P ligands. This should be conveniently observed in the ^{31}P NMR spectra with two doublets anticipated for the two coupled phosphorus environments. However, only the spectrum of **3** gave this pattern ($^2J_{PP} = 6.2$ Hz); ^{31}P NMR spectra of **1**, **2**, **4**, and **6** all returned single ^{31}P resonances, apparently contradicting the crystallographic data. Therefore, variable-temperature ^{31}P NMR experiments were performed. At low temperature the anticipated set of doublets was observed for each complex, thus indicating that a dynamic interchange of the all-*cis* enantiomers is occurring at ambient temperature (Scheme 3).

To probe the mechanism of ligand exchange, kinetic parameters for the averaging process were calculated for **2**−**4** and **6** using line-shape analysis[30] of the ^{31}P NMR data measured over the temperature range 203–363 K in toluene-d_8; selected ^{31}P NMR spectra and calculated exchange rates are shown in Figure 3, and activation parameters are in Table 2. Significantly, for each complex a negative entropy of activation was obtained, suggesting that rearrangement of the ligands occurs via a nondissociative mechanism.[31] There are two possible nondissociative pathways for the interconversion of all-*cis* enantiomers in $(O,P)_2MCl_2$ complexes;[32,33] these are shown in Figure 4.

The first involves a 120° rotation about an O,P,Cl trigonal face with the two chelate rings confined to each face (C_{2v}-symmetric transition state); the second requires a 120° rotation about the P,P,Cl face with the chelate rings spanning the two trigonal faces (C_s-symmetric transition state). These mechanisms are not distinguishable by NMR spectroscopy. What is clear is that the rate of this rearrangement is determined by the steric bulk of the substituents *ortho* to the phenoxide donors, with **2**, bearing phenyl substituents, exchanging 100 times faster at 303 K than **3**, which contains *tert*-butyl groups (this difference is almost entirely entropic). Otherwise the separation of the trigonal faces, determined by the radii of the metal centers (Ti < Zr > Hf), appears to play a key role in controlling the rate of ligand exchange.

The NMR spectra of **5** afforded a single set of resonances for the O,P ligands in accord with the ground-state structure established by crystallography.[25] Comparable spectra were obtained at 323 and 223 K, indicating a nonfluxional structure.

Ethylene Polymerization Studies. Complexes **1**−**6** were investigated as catalysts for ethylene polymerization[34] using methylaluminoxane (MAO) as the cocatalyst; activity and molecular weight data are collected in Table 3. The productivities of the titanium catalysts, **1**−**3**/MAO, are clearly improved when a bulky substituent is positioned *ortho* to the phenoxide donor. Increasing bulk also gives order of magnitude increases in molecular weight with concurrent decreases in the polydispersity index (PDI). Similar observations have been noted by Fujita et al. for phenoxyimine catalyst systems.[3] Analyses of the polymer by ^{13}C NMR spectroscopy revealed highly linear polyethylene (PE). Also visible in the polymer samples isolated using **1**/MAO and **2**/MAO were signals for *n*-alkyl end-groups, consistent with chain transfer to aluminum operating as the predominant termination mechanism.

The zirconium catalyst **4**/MAO was found to have exceptional activity for ethylene polymerization with submicromolar quantities of catalyst required to prevent excessive exotherms and polymer yields. At reduced precatalyst loadings the concentration of cocatalyst also had to be reduced to achieve optimal activity. At a precatalyst loading of 40 nmol and employing 0.75 mmol of MAO, an optimized activity of 49 000 g/mmol·h·bar was recorded over 60 min, with a molecular weight (M_n) of 16.6 kg/mol. Altering the phosphine substituents from phenyl to isopropyl resulted in a dramatic lowering of the productivity and a very broad molecular weight distribution. Although care must be exercised when extrapolating metal–ligand geometries from precatalysts to the active species, the differing configurations of **4** (all-*cis*) and **5** (P-*trans*) may be responsible for this clear change in performance. We shall return later to scrutinize the nature of the active species derived from **4**. The polyethylene from both zirconium catalysts showed evidence for chain transfer to aluminum in their ^{13}C NMR spectra.

(28) The molecular structure of **5**, reported in ref 25, has folded C_2OPZr rings with the metal lying ca. 0.29 and ca. 0.36 Å out of the rest of the chelate.

(29) The chlorine, phosphorus, and oxygen atoms of the coordination sphere in **6** have been renumbered with respect to the report in ref 25 in order to match the numbering of the atoms in the structures reported here. Cl(1) and Cl(2) have swapped, as have P(1) and P(2), and O(1) and O(2).

(30) Reich, H. J. *WINDNMR* v7.1.6, 2002. For full kinetic data and Eyring plots see the Supporting Information.

(31) Non-dissociative pathways have been proposed in other octahedral bis-bidentate Group 4 metal complexes: (a) Fay, R. C.; Lindmark, A. F. *J. Am. Chem. Soc.* **1983**, *105*, 2118. (b) Rahim, M.; Taylor, N. J.; Xin, S.; Collins, S. *Organometallics* **1998**, *17*, 1315. (c) Kakaliou, L.; Scanlon, W. J.; Qian, B.; Baek, S. W.; Smith, M. R.; Motry, D. H. *Inorg. Chem.* **1999**, *38*, 5964. (d) Otten, E.; Dijkstra, P.; Visser, C.; Meetsma, A.; Hessen, B. *Organometallics* **2005**, *24*, 4374.

(32) (a) Bickley, D. G.; Serpone, N. *Inorg. Chem.* **1976**, *15*, 948. (b) Bickley, D. G.; Serpone, N. *Inorg. Chem.* **1976**, *15*, 2577.

(33) Bailar, J. C. *J. Inorg. Nucl. Chem.* **1958**, *8*, 165.

(34) After all polymerizations the reaction medium was examined by GC. No oligomeric products were detected in any instance.

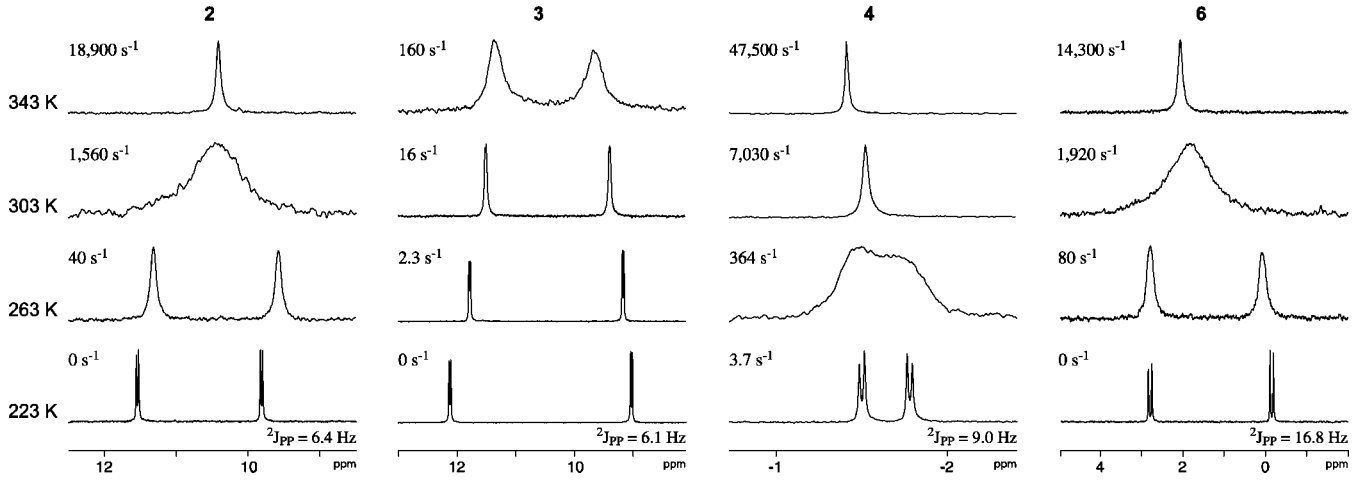

Figure 3. Selected variable-temperature ^{31}P NMR spectra (toluene-d_8) for **2**−**4** and **6** with associated exchange rates.

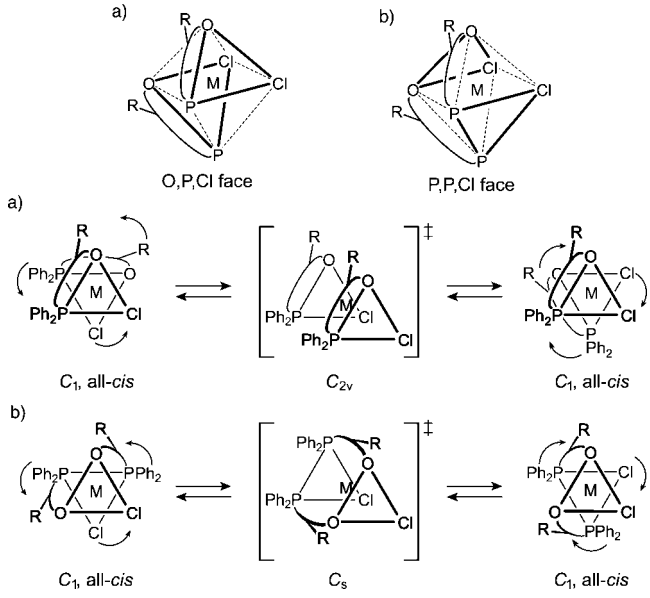

Figure 4. Nondissociative pathways for ligand exchange in bis(phosphanylphenoxide)MCl_2 complexes.

Table 2. Activation Parameters for the Ligand Exchange in 2−4 and 6 (toluene-d_8 solvent)

complex (M, R)	$\Delta H^{\ddagger}$ (kcal/mol)	$\Delta S^{\ddagger}$ (cal/K·mol)	$\Delta G^{\ddagger}_{298K}$ (kcal/mol)
2 (Ti, Ph)	13.2(2)	−0.6(5)	13.4(4)
3 (Ti, ^{t}Bu)	12.3(2)	−12.6(5)	16.1(3)
4 (Zr, ^{t}Bu)	11.5(2)	−3.4(6)	12.5(3)
6 (Hf, ^{t}Bu)	10.8(1)	−8.3(5)	13.3(3)

The hafnium catalyst **6**/MAO also showed a marked sensitivity to the quantity of cocatalyst, with an optimized productivity of 2000 g/mmol·h·bar. In all cases the polymer had a broad multimodal molecular weight distribution. It is also of note that polymerizations using **6**/MAO were accompanied by significant induction times, with the vast majority of the polymer being formed in the final 30 min. Since aging a solution of **6**/MAO (100 equiv) for 30 min prior to injection into the polymerization vessel did not improve the productivity, or reduce the induction time, it is proposed that insertion into the initially formed Hf−Me bonds is rate-limiting.[35] Furthermore, ^{13}C NMR analysis of the polymer revealed that termination occurs by chain transfer to aluminum, which regenerates Hf−Me bonds and hence further limits insertion. As aluminum methyls are steadily consumed, the rate at which Hf−Me bonds are formed should decrease, resulting in an increased ethylene uptake as the run progresses.

Since chain transfer to aluminum appears to occur readily for these catalysts, we decided to investigate **4** and **6** as candidates for the catalyzed chain growth (CCG) of short chain linear alkanes using $ZnEt_2$ as the chain transfer agent.[36] Polymerizations in the presence or absence of $ZnEt_2$ are collected in Table 4. For both catalysts introducing $ZnEt_2$ to the reaction mixture gave a significant decrease in molecular weight and narrow molecular weight distributions (PDI 1.2–1.3) consistent with efficient CCG. Also of note was the considerable increase in the productivity of **6**/MAO. This is consistent with the previous assertion that insertion into Hf−Me bonds is rate-limiting. In the presence of $ZnEt_2$ rapid alkyl exchange generates Hf−Et bonds into which ethylene readily inserts. Additional CCG reactions in which samples were taken at intervals through the run and the products analyzed by GC revealed Poisson distributions of PE oligomers that increased in molecular weight over time; selected distributions for **4** are shown in Figure 5 (all distributions can be found in the Supporting Information).

Propylene Polymerization Studies. Complexes **4** and **6** also showed significant productivities for the polymerization of propylene using "dried"-MAO[37] (DMAO) as the cocatalyst (see Table 5). At 20 °C **4**/DMAO gave a viscous oil of moderate molecular weight and low PDI with a productivity of 5340 g/mmol·h·bar. Analysis of the polymer by ^{13}C NMR spectroscopy (Figure 6) showed it to have a slight syndiotactic bias ([*rr*] = 38.5%; cf. 25.0% for atactic polymer). Full pentad

(35) (a) Wester, T. S.; Johnsen, H.; Kittilsen, P.; Rytter, E. *Macromol. Chem. Phys.* **1998**, *199*, 1989. (b) Liu, Z.; Somsook, E.; White, C. B.; Rosaaen, K. A.; Landis, C. R. *J. Am. Chem. Soc.* **2001**, *123*, 11193.

(36) (a) Britovsek, G. J. P.; Cohen, S. A.; Gibson, V. C.; Maddox, P. J.; van, Meurs *Angew. Chem., Int. Ed.* **2002**, *41*, 489. (b) Britovsek, G. J. P.; Cohen, S. A.; Gibson, V. C.; van Meurs, M. *J. Am. Chem. Soc.* **2004**, *126*, 10701. (c) van Meurs, M.; Britovsek, G. J. P.; Gibson, V. C.; Cohen, S. A. *J. Am. Chem. Soc.* **2005**, *127*, 9913. (d) Arriola, D. J.; Carnahan, E. M.; Hustad, P. D.; Kuhlmann, R. L.; Wenzel, T. T. *Science* **2006**, *312*, 714. (e) Kempe, R. *Chem.−Eur. J.* **2007**, *13*, 2764.

(37) DMAO is MAO with residual $AlMe_3$ removed under vacuum (see Supporting Information). DMAO has been shown to improve the performance of several non-metallocene catalysts: (a) Hasan, T.; Ioku, A.; Nishii, K.; Shiono, T.; Ikeda, T. *Macromolecules* **2001**, *34*, 3142. (b) Hagimoto, H.; Shiono, T.; Ikeda, T. *Macromol. Rapid Commun.* **2002**, *23*, 73. (c) Furayama, R.; Saito, J.; Ishii, S.; Mitani, M.; Matsui, S.; Tohi, Y.; Makio, H.; Matsukawa, N.; Tanaka, H.; Fujita, T. *J. Mol. Catal. A: Chem.* **2003**, *200*, 31.

Table 3. Ethylene Polymerization Results for Complexes 1−6[a]

precatalyst (loading (μmol))	MAO loading (mmol)	yield PE (g)	activity[b]	M_n[c] (kg/mol)	M_w[c] (kg/mol)	M_w/M_n
1 (5.0)	2.50	0.41	41	1.9	529	278[d]
2 (5.0)	2.50	6.15	615	19.2	44.5	2.3
3 (5.0)	2.50	3.90	390	782	1,370	1.8
4 (0.1)	2.50	2.24	11 200	8.2	21.0	2.6
4 (0.1)	1.25	5.34	26 700	12.0	71.8	6.0
4 (0.1)	0.75	5.00[e]	100,000[e]	13.1	54.3	4.1
4 (0.04)	0.75	3.92	49 000	16.6	143	8.6
5 (5.0)	2.50	0.35	35	1.0	109	109[f]
6 (1.0)	2.50	1.10	550	1.0	8.3	8.3[g]
6 (1.0)	1.25	2.13	1070	2.0	228	114[h]
6 (1.0)	0.75	4.00	2000	6.6	580	88[i]

[a] Conditions: 400 mL glass reactor, mechanical stirring, toluene (200 mL), 2 bar ethylene, 25 °C, 1 h (except *e*). [b] Activities in g/mmol·h·bar. [c] Determined by high-throughput GPC. [i] Trimodal: M_{pk} = 1.7, 51.5, and 899 kg/mol. [h] Trimodal: M_{pk} = 1.2, 18.6, and 562 kg/mol. [d] Multimodal: M_{pk} = 1.5 kg/mol. [e] Run time 15 min. [f] Bimodal: M_{pk} = 0.5 and 25.9 kg/mol. [g] Bimodal: M_{pk} = 0.6 and 10.5 kg/mol.

Table 4. CCG on $ZnEt_2$ Using 4 and 6[a]

precatalyst (loading (μmol))	$ZnEt_2$ loading (mmol)	yield (g)	activity[b]	M_n[c](g/mol)	M_w[c](g/mol)	M_w/M_n
4 (0.5)	0	1.05	25 200	2600	13 900	5.3
4 (0.5)	4	1.25	30 000	250	300	1.2
6 (1.5)	0	0.17	461	800	3000	3.8
6 (1.5)	4	3.75	10 000	300	400	1.3

[a] Conditions: Schlenk, magnetic stirring, MAO (1 mmol), toluene (100 mL), 1 bar ethylene, 25 °C, 5 min (**4**)/15 min (**6**). [b] Activities in g/mmol·h·bar. [c] Determined by high-throughput GPC.

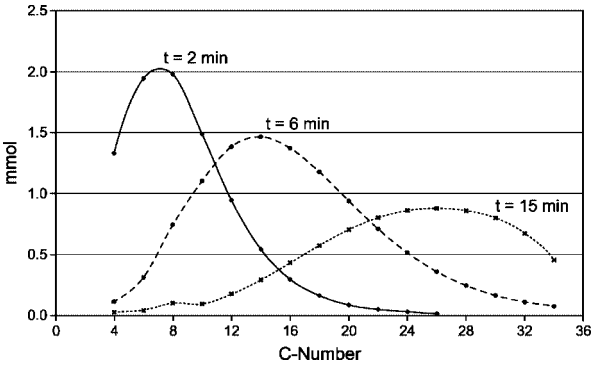

Figure 5. Oligomer distributions from **4**/MAO with $ZnEt_2$.

analysis[38] indicates this selectivity is induced by chain-end control, with the probability of a *rac* insertion (P_r) at 61.7%. No chain end-groups were visible in the NMR spectrum of the polymer. By lowering the polymerization temperature to −20 °C, and hence increasing the concentration of propylene in solution, the activity of **4**/DMAO was increased to 7010 g/mmol·h·bar. At −30 and −50 °C activities decreased, indicating that insertion becomes rate-limiting. At lower temperatures stereoselectivities did improve slightly; for example at −50 °C P_r = 65.9%. A polymerization in liquid propylene at room temperature[39] gave a productivity of 13 300 g/mmol·h, which is among the highest reported productivities for a post-metallocene propylene polymerization system. By using MAO as the cocatalyst the molecular weight of the polymer could be decreased such that isobutyl end-groups became visible in the ^{13}C NMR spectrum.[40] This not only indicates that chain transfer to aluminum operates but that insertion occurs in a 1,2-fashion (Scheme 4).

Consistent with the observations for ethylene polymerization, **6**/DMAO (772 g/mmol·h·bar at 25 °C) gave a somewhat lower productivity than **4**/DMAO, but this could be increased, to 949 g/mmol·h·bar, by raising the polymerization temperature to 50 °C. Again the polymer was isolated as a viscous oil, with NMR analysis revealing a reduced level of stereocontrol (P_r = 56.2% at 25 °C) and isobutyl end-groups.

Toward the Active Species. In order to rationalize the stereoselectivity of **4**/DMAO for propylene polymerization, more information was required on the structure of the catalytically active species. Treating $ZrBn_4$ (Bn = CH_2Ph) with 2 equiv of 6-(*tert*-butyl)-2-diphenylphosphanylphenol, or reacting **4** with 2 equiv of BnMgBr, gave the dibenzyl complex **7** as an analytically pure air- and moisture-sensitive yellow solid (Scheme 5).

Recrystallization from heptane yielded crystals suitable for an X-ray structure determination. The molecular structure (Figure 7) revealed an geometry analogous to that found for its dichloride relative **4**, with the oxygen, phosphorus, and carbon donor atoms all lying mutually *cis*. The geometry at the metal center is a little more distorted from octahedral for **7**, the *cis* angles ranging between 65.70(8)° and 112.86(11)° (cf. 68.86(5)–103.30(2)° in **4**) and the two most acute angles being associated with the bites of the O,P ligands (Table 6). The P(2)/O(2) five-membered C_2OPZr chelate ring is again flat, all five atoms being coplanar to within ca. 0.02 Å, while the P(1)/O(1) ring has an envelope conformation, the metal lying ca. 0.53 Å out of the C_2OP plane (which is coplanar to within ca. 0.01 Å) in the direction of O(2). Despite the change from chloride to benzyl ligands, the pattern of Zr−P and Zr−O bonding is similar, with Zr−P(1) longer than Zr−P(2) (carbon vs oxygen in the *trans* position) and Zr−O(2) longer than Zr−O(1) (carbon vs phosphorus in the *trans* position). For the two benzyl ligands, Zr−C(8) (*trans* to oxygen) is longer than Zr−C(1) (*trans* to phosphorus). There is no evidence of any multiple bonding between the benzyl ligand and the metal center.

The room-temperature solution-state NMR spectra of **7** revealed broad peaks for the benzyl and *tert*-butyl protons, indicative of a complex with an intermediate rate of O,P ligand exchange (Figure 8). Additionally, a sharp peak in the *tert*-butyl region suggested that a more rigid geometric isomer might also

(38) Pentad intensities determined by line fitting using MestReC v4.7.0.0. These were compared to best-fit chain-end and enantiomorphic site control models. (a) Busico, V.; Cipullo, R. *Prog. Polym. Sci.* **2001**, *26*, 443. (b) Bovey, F. A.; Tiers, G. V. D. *J. Polym. Sci.* **1960**, *44*, 173. (c) Shelden, R. A.; Fueno, T.; Tsunetsugu, T.; Furukawa, J. *J. Polym. Sci., Part B* **1965**, *3*, 23.

(39) Conditions: 1 L steel autoclave, mechanical stirring, **4** (1 μmol), MAO (2.5 mmol), 500 mL of liquid propylene, 25 °C, 1 h.

(40) Polymerization conditions: as for Table 5 except MAO (5.0 mmol) used as cocatalyst. See Supporting Information for ^{13}C NMR spectrum.

Table 5. Propylene Polymerizations Using 4 and 6[a]

precatalyst (loading (μmol))	temp (°C)	activity[b]	M_n[c](kg/mol)	M_w[c](kg/mol)	M_w/M_n	[*rr*][d](%)
4 (2.5)	20	5,340	37.0	62.7	1.70	38.5
4 (2.5)	−20	7,010	52.9	79.1	1.49	40.5
4 (2.5)	−30	4,500	58.4	95.5	1.63	42.1
4 (2.5)	− 50[e]	1,750[e]	18.3	28.4	1.6	44.6
6 (10.0)	50	949	14.9	34.4	2.30	33.7
6 (10.0)	25	772	18.2	35.1	1.93	36.0
6 (10.0)	0	112	7.79	12.7	1.63	37.3

[a] Conditions: Schlenk, magnetic stirring, DMAO (2.5 mmol), TIBAL (125 μmol), heptane (100 mL) (except *e*), 2 bar propylene, 30 min (**4**)/1 h (**6**). [b] Activities in g/mmol·h·bar (except *e*). [c] Determined by GPC. [d] Determined by ^{13}C NMR (101 MHz). [e] Liquid propylene (100 ml); activity in g/mmol·h.

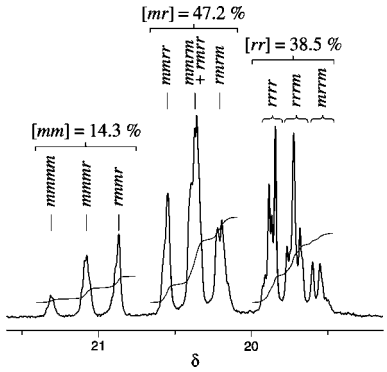

Pentad	LF[a]	CE[b]
mmmm	1.6	2.2
mmmr	6.0	6.9
rmmr	6.3	5.6
mmrr	9.8	11.2
mmrm + *rmrr*	25.4	24.9
rmrm	12.5	11.2
rrrr	14.4	14.5
rrrm	17.3	18.0
mrrm	6.6	5.6

Figure 6. ^{13}C NMR (101 MHz, methyl region) of polypropylene formed with **4**/DMAO at 20 °C, with pentad analysis. [a]From line-fitting analysis. [b]Calculated for chain-end control (P_r = 61.7%).

Scheme 4. Isobutyl-Terminated Polymer from 1,2-Propylene Insertions and Chain Transfer to Aluminum

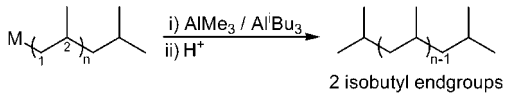

Scheme 5. Synthesis of a Bis(phosphanylphenoxide) Zirconium Dibenzyl Complex

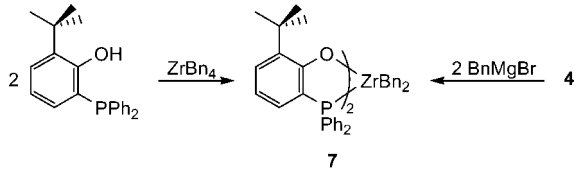

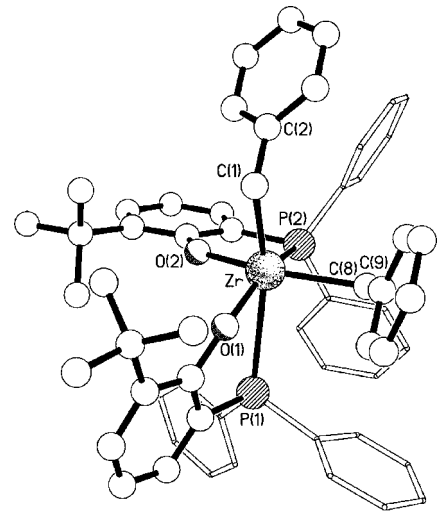

Figure 7. Molecular structure of **7**.

Table 6. Selected Bond Lengths (Å) and Angles (deg) for 7

Zr−O(1)	1.981(3)	Zr−O(2)	2.013(3)
Zr−P(1)	3.0194(11)	Zr−P(2)	2.8583(10)
Zr−C(1)	2.277(4)	Zr−C(8)	2.310(4)
P(1)−Zr−C(1)	160.56(11)	P(2)−Zr−C(1)	112.86(11)
P(2)−Zr−O(1)	149.73(8)	P(2)−Zr−C(8)	79.59(11)
O(2)−Zr−C(8)	147.94(13)	O(1)−Zr−C(8)	107.34(14)
P(1)−Zr−P(2)	85.47(3)	O(1)−Zr−C(1)	95.09(13)
O(1)−Zr−O(2)	99.10(11)	O(2)−Zr−C(1)	94.55(14)
C(1)−Zr−C(8)	100.73(17)	P(1)−Zr−O(1)	65.70(8)
P(1)−Zr−O(2)	86.06(8)	P(2)−Zr−O(2)	68.49(7)
P(1)−Zr−C(8)	88.53(12)		

be present. The room-temperature ^{31}P NMR spectrum revealed broad signals of approximately equal intensity at 2.3 and −9.3 ppm, consistent with inequivalent but exchanging phosphorus environments in the all-*cis* structure. However, the spectrum also included a very broad peak at 5 ppm and a sharper signal at −14.6 ppm. It is proposed that these peaks are due to *trans*-O_2 and *trans*-P_2 geometric isomers. To probe whether this mixture could be converted to a single geometric product, a sample of **7** in C_6D_6 was heated to 50 °C for 2 h. No change in the isomer distribution was observed. It is also of note that the ratio of the isomers was dependent on the synthetic route employed, with a greater proportion of the all-*cis* isomer formed using BnMgBr (ca. 80% compared to ca. 53% using $ZrBn_4$). Therefore, the observed distribution is not an interchanging equilibrium mixture but rather represents a kinetic distribution of products.

On cooling to 223 K, the broad signal at 5 ppm in the ^{31}P NMR spectrum sharpened to a singlet. Additionally, the broad signals assigned to the all-*cis* isomer resolved to two sharp doublets ($^2J_{PP}$ = 21 Hz), consistent with a configurationally rigid C_1-symmetric complex. The high-field peak does not significantly alter upon cooling and is hence assigned to the *trans*-P_2 isomer by comparison to the variable-temperature behavior of **5**. The low-temperature ^{1}H NMR spectrum of **7** includes five distinct benzyl signals in the region 1.9–3.0 ppm. Four of these are of equal intensity and are assigned to the four inequivalent benzyl protons of the all-*cis* isomer.[41] It was anticipated that the benzyl protons of the *trans*-O_2 and *trans*-P_2 structures should give at least two signals. Since only one benzyl signal (2.68 ppm) remains unassigned, it is proposed that these two isomers have benzyl signals with coincidental chemical shifts. It should be noted that the low-temperature ^{13}C NMR spectrum contains four signals for the benzylic carbons (64–74 ppm) and the quaternary carbon of the *tert*-butyl groups (34–35 ppm), consistent with there being one C_1- and two C_2-symmetric isomers.

The activation parameters for O,P ligand exchange in the all-*cis* isomer of **7** ($\Delta H^{\ddagger}$ = 10.5(3) kcal/mol, $\Delta S^{\ddagger}$ = −10.4(9) cal/

(41) A COSY spectrum revealed cross-peaks for the peaks at 2.93 and 1.95 ppm and at 2.33 and 2.17 ppm, indicating that each pair is bound to the same benzylic carbon.

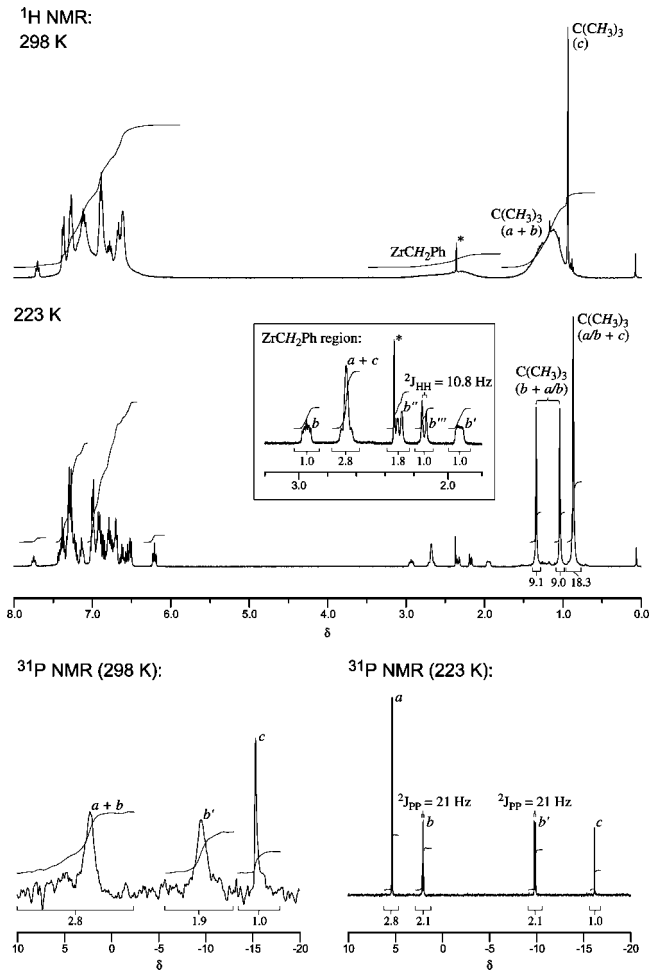

Figure 8. Variable-temperature ^{1}H and ^{31}P NMR spectra of **7** (from $ZrBn_4$) in $CDCl_3$; * = residual toluene; *a* = *trans*-O_2, *b* = all-*cis*, *c* = *trans*-P_2 geometric isomer.

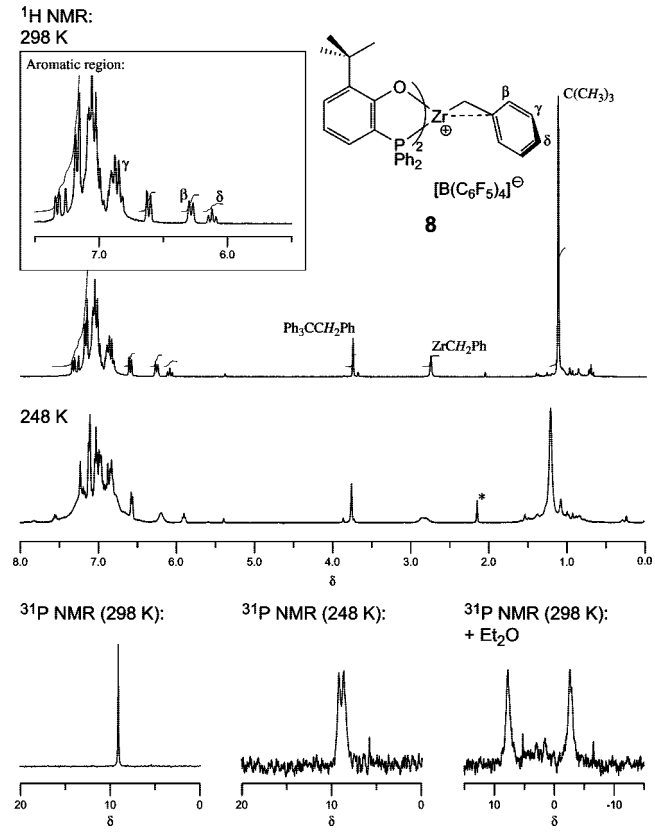

Figure 9. Variable-temperature ^{1}H and ^{31}P NMR spectra of **8** in C_6D_5Br. * = residual toluene.

K·mol, $\Delta G^{\ddagger}_{298K}$ = 13.6(6) kcal/mol) were obtained using the same methodology as for the dichloro complexes.[30] Again, negative $\Delta S^{\ddagger}$ values are indicative of a nondissociative process. Predictably, given the increased steric influence of the benzyl ligands compared to chlorides, the rate of isomerization was considerably slower than in **4** (approximately 7-fold at 298 K).

Of the reagents that can be used to abstract alkyl groups, $[Ph_3C][B(C_6F_5)_4]$ is particularly attractive since both the borate anion and eliminated hydrocarbon are typically noncoordinating, thus facilitating study of the base-free cation.[42] Hence, **7** was treated with 1 equiv of $[Ph_3C][B(C_6F_5)_4]$ at room temperature in an NMR-scale reaction in C_6D_5Br. Near-quantitative formation of the cationic benzyl complex **8** was observed in the ^{1}H NMR spectrum (Figure 9), which included two equimolar signals assignable to the CH_2 groups of the zirconium-bonded benzyl (2.84 ppm) and the eliminated 1,1,1,2-tetraphenylethane (3.82 ppm). Also of note are the relatively high-field shifts for the aromatic protons of the benzyl ligand (6.12–6.64 ppm), suggesting η^2-coordination. Further evidence for this bonding mode was provided by a ^{1}H-coupled ^{13}C NMR spectrum, which included a triplet at 79.3 ppm for the benzylic carbon with a $^1J_{CH}$ value of 148 Hz.[43,44] Only one $C(CH_3)_3$ signal and one phosphorus signal are observed in the ^{1}H and ^{31}P NMR spectra, respectively, indicating that the cation is either highly fluxional or adopts a square-based pyramidal structure with the benzyl ligand in the apical position. At low temperature the ^{1}H NMR spectrum significantly broadens and the ^{31}P NMR spectrum reveals two distinct, though broad, resonances indicative of a C_1-symmetric ground state akin to the parent six-coordinate complex **7**. To further probe the structure of **8**, a small amount of ether was added to the NMR sample. The room-temperature ^{31}P NMR then contained two separate, equal intensity signals at 8.3 and −2.1 ppm, consistent with a six-coordinate ether complex in which trigonal face rotation is restricted by the additional steric constraints imposed by binding of a molecule of diethyl ether. Near-identical ^{19}F NMR spectra were obtained with or without ether coordination, consistent with $B(C_6F_5)_4^-$ acting as a noncoordinating counterion.

An analogous cationic species **8′** could be obtained upon treatment of **7** with 50 equiv of DMAO in C_6D_6 (Figure 10). The ^{1}H NMR spectrum clearly shows signals for an η^2-bound benzyl moiety, and the ^{31}P NMR spectrum reveals a sharp singlet almost identical to that seen for **8**. Analogous NMR-scale experiments were performed using the dichloride complex

(42) Coordination of solvent cannot typically be ruled out. A chlorobenzene adduct of a zirconium benzyl cation has been structurally characterized: Wu, F.; Dash, A. K.; Jordan, R. F. *J. Am. Chem. Soc.* **2004**, *126*, 15360.

(43) Values above 130 Hz indicate some distortion of the benzyl ligand. Examples of Zr complexes in which a solution state η^2-interaction has been confirmed by X-ray analysis include: (a) Tsurugi, H.; Matsuo, Y.; Yamsgata, T.; Mashima, K. *Organometallics* **2004**, *23*, 2797. (b) Shao, P.; Gendron, R. A. L.; Berg, D. J.; Bushnell, G. W. *Organometallics* **2000**, *19*, 509. (c) Bei, X. H.; Swenson, D. C.; Jordan, R. F. *Organometallics* **1997**, *16*, 3282. (d) Crowther, D. J.; Borkowsky, S. L.; Swenson, D.; Meyer, T. Y.; Jordan, R. F. *Organometallics* **1993**, *12*, 2897. (e) Jordan, R. F.; Lapointe, R. E.; Bajgur, C. S.; Echols, S. F.; Willett, R. *J. Am. Chem. Soc.* **1987**, *109*, 4111. (f) Latesky, S. L.; McMullen, A. K.; Niccolai, G. P.; Rothwell, I. P.; Huffman, J. C. *Organometallics* **1985**, *4*, 902.

(44) It has recently been suggested that in the absence of coordinated solvent benzyl ligands may in fact bind in an η^3 manner: Sassmannshausen, J.; Track, A.; Stelzer, F. *Organometallics* **2006**, *25*, 4427.

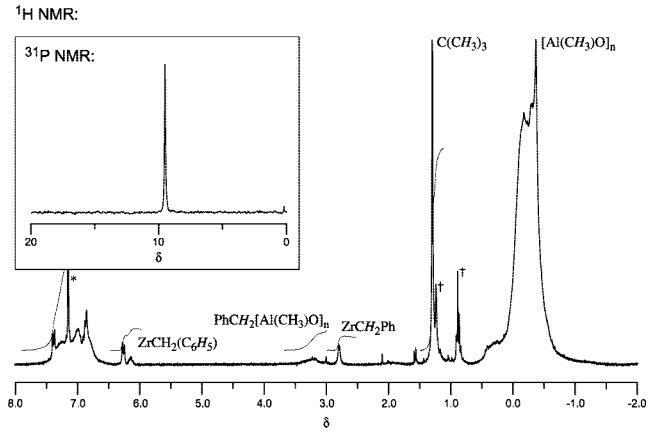

Figure 10. ^{1}H and ^{31}P NMR spectra of **8′** (**7** + DMAO) in C_6D_6 (*). † = residual heptane in DMAO.

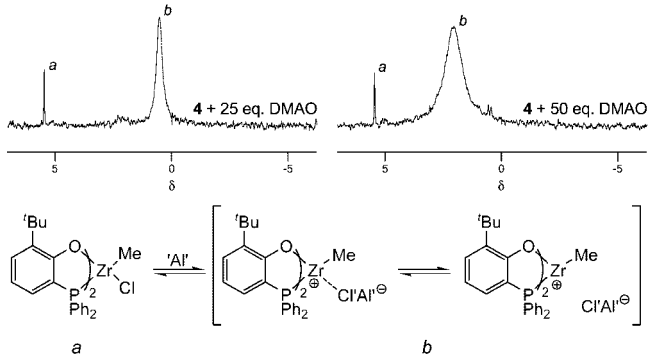

Figure 11. ^{31}P NMR spectra of **4** + DMAO in C_6D_6.

4 with differing amounts of DMAO. The ^{31}P NMR spectra reveal a low-intensity sharp signal and a larger broad peak (Figure 11). The low-intensity signal is tentatively assigned to a $(O,P)_2Zr(Me)Cl$ complex and the broad peak to $(O,P)_2Zr^+Me$. In the absence of the additional alkyl−metal interactions seen for **8**/**8′** it is proposed that the aluminoxane anion can reversibly access the zirconium center. Such dynamic interactions, and the nonuniform nature of aluminoxanes, can hence explain the observed broadening.[45] Increasing the concentration of DMAO increases both the yield of the cationic species and the likelihood of cation–anion interactions.

Interestingly, when a solution of **8** (formed using $[Ph_3C][B(C_6F_5)_4]$) was placed under an atmosphere of ethylene, the yellow color was retained[46] and no polymer was formed, suggesting that the η^2-benzyl interaction is too strong to be displaced by ethylene.[47] This was reproduced under polymerization conditions (Table 7) with no polymer formed at 25 °C. However, running the polymerization at 50 °C did give polymer, suggesting that an $\eta^2-\eta^1$ rearrangement may occur at elevated temperature. Furthermore, polymer could be formed at room temperature using MAO as the cocatalyst, with a steady increase in ethylene uptake measured throughout the run. This suggests gradual exchange of the η^2-benzyl ligands for methyls by the $AlMe_3$ present in the cocatalyst.

Given the fluxional nature of the catalytically active species derived from **4** or **7** it is perhaps less surprising that the polypropylene formed is virtually atactic. However, it should be noted that there are fluxional zirconocenes that can form isotactic−atactic stereoblock polymers.[48] Furthermore, the highly syndiotactic polymer generated using bis(phenoxy-imine)titanium catalysts is thought to be a direct consequence of an isomerization process that occurs after each monomer insertion.[49] For a fluxional catalyst to give stereoenriched PP via an enantiomorphic site control mechanism, two requirements must be met. First, the ground-state structure(s) must be able to influence the orientation of the polymer chain in order to control the mode of monomer insertion. Second, the rate of geometrical isomerization must be comparable to, but preferably less than, the rate of insertion. Assuming that the O,P ligand framework in **4**/DMAO can control monomer insertion, this means the rate of ligand reorganization must be slower than the rate of monomer insertion, which is calculated as 71 s^{-1} at 20 °C.[50] A crude comparison with the ligand exchange rates calculated for **4** and **7** (3400 and 596 s^{-1}, respectively) indicates that the fluxional processes in **4**/DMAO are too rapid for any stereocontrol to be imparted.

Table 7. Ethylene Polymerizations with 7[a]

cocatalyst[b]	temp (°C)	yield PE (g)	activity[c]	M_n[d] (kg/mol)	M_w[d] (kg/mol)	M_w/M_n
TB	25	0.00	0			
TB	50	1.56	3900	6.3	16.2	2.6
MAO	25	2.79	14 000	7.8	20.6	2.6

[a] Conditions: glass reactor, mechanical stirring, **7** (0.2 μmol), MAO (2.5 mmol) or $[Ph_3C][B(C_6F_5)_4]$ (0.2 μmol) and Al^iBu_3 (0.5 mmol), toluene (200 mL), 2 bar ethylene, 1 h (TB)/30 min (MAO). [b] TB = $[Ph_3C][B(C_6F_5)_4]$. [c] Activities in g/mmol·h·bar. [d] Determined by GPC vs PS standards.

Conclusions

A number of bis(phosphanylphenoxide) group 4 metal complexes have been synthesized in order to assess the effect of incorporating phosphine donors into early transition metal based olefin polymerization catalysts. The geometries of these complexes are dependent upon the phosphine substituents, with diisopropyl- and diphenyl-phosphine zirconium derivatives possessing *trans*-P_2 and all-*cis* structures, respectively.

Polymerization studies have highlighted a *tert*-butyl-substituted zirconium catalyst that shows excellent activity in the production of polyethylene and polypropylene. In fact this catalyst is one of the most active post-metallocene catalysts reported to date, suggesting that there is considerable scope for utilizing the combination of hard donors with soft phosphine donors in early transition metal polymerization catalysis. It can be expected that linking the O,P ligands to one another might increase the configurational stability of the catalyst, which may then offer the possibility for stereoselective α-olefin polymerizations.

Experimental Methods

The synthesis of the phosphanylphenols, phosphanylphenoxides, and complexes **1**−**6** has been reported elsewhere.[25] $ZrBn_4$ was synthesized according to a published procedure.[51] Air-sensitive procedures were performed under nitrogen using standard Schlenk techniques, with solvents being distilled over standard drying agents

(45) Hawrelak, E. J.; Deck, P. A. *Organometallics* **2003**, *22*, 3558.
(46) Kress et al. have observed a single ethylene insertion, indicated by a lack of polymer coupled with a loss of color: Gauvin, R. M.; Osborn, J. A.; Kress, J. *Organometallics* **2000**, *19*, 2944.
(47) Bochmann, M.; Lancaster, S. J. *Organometallics* **1993**, *12*, 633.
(48) Lin, S.; Waymouth, R. M. *Acc. Chem. Res.* **2002**, *35*, 765.
(49) Miliano, G.; Cavallo, L.; Guerra, G. *J. Am. Chem. Soc.* **2002**, *124*, 13368.
(50) Insertion rate (s^{-1}) = polymer yield (g)/[fw(propylene) (g/mol) × cat. loading (mol) × run time (s)].
(51) Felten, J. J.; Anderson, W. P. *J. Organomet. Chem.* **1972**, *36*, 87.

and degassed before use. Deuterated solvents were dried and stored over 4 Å molecular sieves. Ethylene (CP grade) and propylene (instrument grade) were purified by passing them through an Oxytrap and a gas drier (Alltech Associates). Compounds were analyzed by NMR: Bruker AC-250, Bruker DRX-400, or Bruker Avance-600 spectrometers (referenced to solvent resonances for ^{1}H and ^{13}C NMR, and externally to 85% $H_3PO_{4(aq)}$ and $CFCl_3$ for ^{31}P and ^{19}F NMR, respectively). IR: Perkin-Elmer 1760X FT-IR. Mass spectrometry: Autospec Q spectrometer. Elemental analyses were performed at London Metropolitan University. Polymer samples were analyzed by ^{13}C NMR: Bruker Avance-400 spectrometer (in 2:1 (by weight) 1,2,4-$C_6H_3Cl_3$:1,1,2,2-$C_2D_2Cl_4$ at 130 °C using a pulse delay of 15 s). GPC (polyethylene): Polymer Laboratories GPC-220 with PLgel HTS-B column (1,2,4-trichlorotoluene, 160 °C, run time = 6 min, PS standards). GPC (polypropylene): Polymer Laboratories LC1220 HPLC pump with two 5 μm (PL gel mixed C 300 × 7.5 mm) columns ($CHCl_3$, 25 °C, run time = 30 min, PS standards).

The numbering scheme below is used in the assignments of the O,P precursors and complexes:

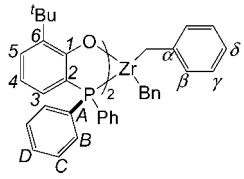

Synthesis of A. To a solution of 1-*tert*-butyl-2-(methoxymethoxy)benzene (14.55 g, 75.0 mmol) in ether (150 mL) was added *n*-butyllithium (30.6 mL, 76.5 mmol), and the mixture was stirred for 12 h. Chlorodiphenylphosphine (14.15 mL, 78.8 mmol) was added to the mixture dropwise at −78 °C. The mixture was stirred at room temperature for 3 h and then filtered. The filtrate was concentrated to dryness and the residue dissolved in THF (75 mL) and 5 M HCl (75 mL). The mixture was stirred and heated at 50 °C for 12 h. The mixture was poured into water (500 mL), filtered, and washed with water (3 × 100 mL). The crude product was triturated in methanol, filtered, and dried under vacuum to give a colorless powder (16.69 g, 41.6 mmol, 56% yield). Anal. Calcd (%) for $C_{23}H_{26}ClO_2P$ (400.88): C, 68.91; H, 6.54. Found: C, 68.87; H, 6.49. ^{1}H NMR (400 MHz, $CDCl_3$): δ 9.40 (br, 1H, Ar-O *H*), 7.74–7.70 (m, 3H, Ar-*H*$_{(4,D)}$), 7.58–7.53 (m, 8H, Ar-*H*$_{(B,C)}$), 7.29 (br, 1H, CH_2O *H*), 7.02 (dt, J = 7.7 Hz, J = 3.6 Hz, 1H, Ar-*H*$_{(5)}$), 6.59 (ddd, $^{3}J_{HP}$ = 13.9 Hz, $^{3}J_{HH}$ = 6.9 Hz, $^{4}J_{HH}$ = 1.4 Hz, 1H, Ar-*H*$_{(6)}$), 5.43 (s, 2H, C H_2OH), 1.47 (s, 9H, C(C H_3)$_3$). ^{13}C{^{1}H} NMR (101 MHz, $CDCl_3$): δ 159.5 (d, $^{2}J_{CP}$ = 3.0 Hz, Ar-*C*$_{(2)}$), 144.7 (d, $^{3}J_{CP}$ = 6.6 Hz, Ar-*C*$_{(3)}$), 135.3 (Ar-*C*$_{(4)}$), 134.5 (Ar-*C*$_{(D)}$), 133.8 (d, $^{2}J_{CP}$ = 9.2 Hz, Ar-*C*$_{(6)}$), 133.2 (d, $^{3}J_{CP}$ = 9.4 Hz, Ar-*C*$_{(C)}$), 130.0 (d, $^{2}J_{CP}$ = 12.0 Hz, Ar-*C*$_{(B)}$), 123.6 (d, $^{3}J_{CP}$ = 13.9 Hz, Ar-*C*$_{(5)}$), 119.3 (d, $^{1}J_{CP}$ = 82.7 Hz, Ar-*C*$_{(A)}$), 109.6 (d, $^{1}J_{CP}$ = 89.4 Hz, Ar-*C*$_{(1)}$), 61.0 (d, $^{1}J_{CP}$ = 62.6 Hz, P *C*H_2OH), 35.3 (*C*(CH$_3$)$_3$), 30.4 (C(*C*H$_3$)$_3$). ^{31}P{^{1}H} NMR (162 MHz, $CDCl_3$): δ 20.9 (s). MS (negative FAB; *m*/*z*): 399 [M]$^-$, 333 [M − Cl − CH_2OH]$^-$, 188 [M − ^{t}Bu-2Ph]$^-$. IR (KBr; cm^{-1}): 3142 (OH), 2868br (OH). Crystals suitable for X-ray analyses were grown from a chloroform solution layered with pentane.

Synthesis of 7. Method 1: A solution of $ZrBn_4$ (0.312 g, 0.68 mmol) in toluene (20 mL) was cooled to −10 °C and a solution of 2-*tert*-butyl-6-diphenylphosphanylphenol (0.477 g, 1.43 mmol) in toluene (20 mL) added dropwise. The mixture was stirred for 30 min at −10 °C and for 30 min at 25 °C. The solvent was removed under vacuum and the residue triturated with pentane (5 mL), filtered, and dried under vacuum to give **7** as a yellow powder (0.547 g, 0.58 mmol, 85% yield). Anal. Calcd (%) for $C_{58}H_{58}O_2P_2Zr$ (940.25): C, 74.09; H, 6.21. Found: C, 73.82; H, 6.10. Three different isomers were detected by NMR analysis: *trans*-O_2 (isomer *a*), all-*cis* (*b*), and *trans*-P_2 (*c*). ^{1}H NMR (400 MHz, $CDCl_3$, 298 K): δ 7.70 (t, J = 8.3 Hz, Ar-*H*), 7.38–6.61 (br m, Ar-*H*), 3.00–1.80 (br, 4H(*a*) + 4H(*b*) + 4H(*c*), C H_2Ph), 1.50–0.80 (br, 18H(*a*) + 18H(*b*), C(C H_3)$_3$), 0.94 (s, 18H(*c*), C(C H_3)$_3$). ^{1}H NMR (400 MHz, $CDCl_3$, 223 K): δ 7.74 (t, J = 7.8 Hz, Ar-*H*), 7.43–7.12 (m, Ar-*H*), 7.02–6.68 (m, Ar-*H*), 6.64–6.50 (m, Ar-*H*), 6.21 (t, J = 8.1 Hz, Ar-*H*), 2.96–2.90 (m, 1H(*b*), C H_2Ph), 2.71–2.64 (m, 4H(*a*) + 4H(*c*), C H_2Ph), 2.33 (d, $^{2}J_{HH}$ = 10.8 Hz, 1H(*b*), C H_2Ph), 2.17 (d, $^{2}J_{HH}$ = 10.8 Hz, 1H(*b*), C H_2Ph), 1.97–1.92 (m, 1H(*b*), C H_2Ph), 1.34 (s, 9H(*a*/*b*), C(C H_3)$_3$), 1.04 (s, 9H(*a*/*b*), C(C H_3)$_3$), 0.87 (s, 18H(*a*/*b*) + 18H(*c*), C(C H_3)$_3$). ^{13}C{^{1}H} NMR (101 MHz, $CDCl_3$, 223 K): δ 169.1, 169.0, 168.9, 168.7, 166.4, 166.1, 147.6, 147.5, 146.0, 145.8, 137.8, 137.3, 137.2, 137.2, 137.1, 134.0, 133.6, 133.6, 133.5, 133.5, 133.3, 133.1, 133.1, 132.8, 132.7, 132.2, 132.1, 131.9, 131.8, 131.6, 131.5, 131.3, 131.2, 131.1, 131.0, 130.8, 130.5, 130.1, 129.9, 129.9, 129.8, 129.4, 129.3, 129.2, 129.0, 128.9, 128.7, 128.4, 128.2, 128.0, 127.9, 127.7, 127.2, 125.5, 125.5, 125.2, 123.7, 123.5, 121.3, 120.7, 120.5, 120.2, 119.7, 119.7, 119.6, 119.4, 119.3, 118.3 (Ar-*C*), 73.9, 73.7, 69.6, 63.5 (*C*H_2Ph), 34.8, 34.7, 34.4, 34.0 (*C*(CH$_3$)$_3$), 29.2, 28.8, 28.3 (C(*C*H$_3$)$_3$). ^{31}P{^{1}H} NMR (162 MHz, $CDCl_3$, 298 K): δ 5.3–2.4 (br, 2P(*a*) + 1P(*b*) [49%]), −9.5 (br, 1P(*b*) [33%]), −15.3 (s, 2P(*c*) [18%]). ^{31}P{^{1}H} NMR (162 MHz, $CDCl_3$, 223 K): δ 5.3 (s 2P(*a*) [35%]), 2.0 (d, $^{2}J_{PP}$ = 21 Hz, 1P(*b*) [27%]), −9.8 (d, $^{2}J_{PP}$ = 21 Hz, 1P(*b*) [27%]), −16.2 (s, 2P(*c*) [11%]).

Method 2: To a solution of **4** (0.301 g, 0.36 mmol) in toluene (30 mL) cooled to −78 °C was added dropwise $PhCH_2MgBr$ (1.24 M in THF; 0.60 mL, 0.74 mmol), giving immediate formation of a yellow solution. The mixture was allowed to warm to room temperature over 12 h, over which time a colorless precipitate was formed. The suspension was filtered through Celite and the solvent then removed under vacuum. The residual yellow oil was triturated with pentane and the resultant precipitate filtered and dried under vacuum to give **7** as a yellow powder (0.181 g, 0.19 mmol, 53% yield). Anal. Calcd (%) for $C_{58}H_{58}O_2P_2Zr$ (940.25): C, 74.09; H, 6.21. Found: C, 73.95; H, 6.10. ^{31}P{^{1}H} NMR (101 MHz, $CDCl_3$, 298 K): δ 2.3 (br, 2P(*a*) + 1P(*b*) [60%]), −9.2 (br, 1P(*b*) [40%]), −15.2 (s, 2P(*c*) [<1%]).

Synthesis of 8. In a nitrogen filled glovebox, a C_6D_5Br solution of $[CPh_3][B(C_6F_5)_4]$ (1 equiv) was added to a C_6D_5Br solution of **7** (1 equiv) at 25 °C. The orange solution was transferred to an NMR tube fitted with a Youngs tap valve. The NMR data was acquired immediately. ^{1}H NMR (250 MHz, C_6D_5Br, 298 K): δ 7.34 (dd, $^{3}J_{HH}$ = 7.4 Hz, $^{2}J_{HH}$ = 1.6 Hz, 2H, Ar-*H*), 7.28–6.98 (m, 34 H, Ar-*H*), 6.93–6.82 (m, 8H + 2H, Ar-*H* + Ar-*H*$_{(\gamma)}$), 6.62 (d, J = 7.8 Hz, 2H, Ar-*H*), 6.28 (d, $^{3}J_{HH}$ = 7.5 Hz, Ar-*H*$_{(\beta)}$), 6.12 (t, $^{3}J_{HH}$ = 7.3 Hz, Ar-*H*$_{(\delta)}$), 3.81 (s, 2H, Ph_3CC H_2Ph), 2.83 (s, 2H, ZrC H_2Ph), 1.22 (s, 18H, C(C H_3)$_3$). ^{1}H NMR (400 MHz, C_6D_5Br, 248 K): δ 7.50–6.40 (br m, 48H, Ar-*H*), 6.24 (br s, Ar-*H*$_{(\beta)}$), 5.94 (br t, $^{3}J_{HH}$ = 7.5 Hz, Ar-*H*$_{(\delta)}$), 3.78 (s, 2H, Ph_3CC H_2Ph), 2.84 (br s, 2H, ZrC H_2Ph), 1.21 (s, 18H, C(C H_3)$_3$). ^{13}C NMR (63 MHz, C_6D_5Br, 298 K): selected δ 165.3 (br, Ar-*C*$_{(1)}$), 150.6 (s, Ar-*C*$_{(\alpha)}$), 79.3 (t, $^{1}J_{CH}$ = 148 Hz, Zr *C*H_2Ph), 35.2 (s, *C*(CH$_3$)$_3$), 29.7 (q, $^{1}J_{CH}$ = 123 Hz, C(*C*H$_3$)$_3$). ^{31}P{^{1}H} NMR (101 MHz, C_6D_5Br, 298 K): δ 9.4 (s). ^{31}P{^{1}H} NMR (162 MHz, C_6D_5Br, 248 K): δ 8.4 + 7.9 (2 unresolved br s). ^{19}F{^{1}H} NMR (235 MHz, C_6D_5Br, 298 K): δ −135.9 (s, *o*-BC_6F_5), −166.4 (t, $^{3}J_{FF}$ = 21.2 Hz, *p*-BC_6F_5), −170.2 (pt, J_{FF} = 18.5 Hz, *m*-BC_6F_5).

The reaction was repeated and two drops of dry Et_2O added to the solution. The NMR data were acquired immediately. ^{1}H NMR (250 MHz, C_6D_5Br, 298 K): selected δ 7.59 (d, $^{3}J_{HH}$ = 7.5 Hz, 2H, Ar-*H*), 7.18–6.40 (br m, 49 H, Ar-*H*), 2.50 (br s, 2H, ZrC H_2Ph). ^{31}P{^{1}H} NMR (101 MHz, C_6D_5Br, 298 K): δ 8.3 (br s), −2.1 (br s). ^{19}F{^{1}H} NMR (235 MHz, C_6D_5Br, 298 K): δ −136.0 (s, *o*-BC_6F_5), −166.6 (t, $^{3}J_{FF}$ = 21.0 Hz, *p*-BC_6F_5), −170.4 (pt, J_{FF} = 18.4 Hz, *m*-BC_6F_5).

Reaction of 7 with DMAO. In a nitrogen-filled glovebox, a C_6D_6 solution of DMAO (50 equiv) was added to a C_6D_6 solution of **7**

(1 equiv) at 25 °C. After 20 min, the pale yellow solution was transferred to an NMR tube fitted with a Youngs tap valve, and NMR data were acquired. ^{1}H NMR (250 MHz, C_6D_6): δ 7.41–6.70 (dd + br m, $^3J_{HH}$ = 6.9 Hz, $^4J_{HH}$ = 2.1 Hz, 33H, Ar-*H*), 6.26 (d, $^3J_{HH}$ = 7.8 Hz, 2H, Ar-$H_{(\beta)}$), 6.14 (t, $^3J_{HH}$ = 6.7 Hz, 1H, Ar-$H_{(\delta)}$), 3.24 (br, 2H, DMAO-C H_2Ph), 2.80 (s, 2H, Zr-C H_2Ph), 1.30 (s, 18H, C(C H_3)$_3$), 0.5 > 23>(−1.0) (br m, Al-C H_3). ^{31}P{^{1}H} NMR (101 MHz, C_6D_6): δ 9.4 (s).

Ethylene Polymerization Procedure. A 400 mL glass Fisher-Porter vessel was dried at 50 °C for 12 h. The Fisher-Porter head, equipped with an injection port (fitted with a rubber septum), pressure gauge, and mechanical stirrer, was flame-dried for 5 min and fitted to the glass vessel. The reactor was then purged with nitrogen for 45 min, charged with solvent, purged with 1 bar of ethylene overpressure for 5 min (to give 2 bar total ethylene pressure), and placed in a room-temperature water bath. Scavenger (MAO or Al^{t}Bu$_3$) was introduced at least 5 min before catalyst injection. A solution of precatalyst (for polymerizations using MAO) or activated catalyst (for polymerizations using [CPh_3][$B(C_6F_5)_4$]) in toluene was introduced via syringe to initiate the polymerization. The reaction mixture was rapidly stirred throughout. Polymerizations were terminated by venting the overpressure followed by addition of 5 mL of 2 M $HCl_{(aq)}$. A sample of the reaction mixture was taken for GC analysis. The solid product was precipitated from the mixture by addition of MeOH (400 mL). After filtration the polymer was washed with a large quantity of MeOH and dried under vacuum at 60 °C for 12 h.

Catalyzed Chain Growth Procedure. A Schlenk, containing 100 mL of toluene and a magnetic stirrer under a nitrogen atmosphere, fitted with a rubber septum was purged with ethylene for 5 min and the overpressure then vented (1 bar total ethylene pressure). MAO and, when required, $ZnEt_2$ were then added. If GC samples were to be taken during the run, then a known quantity of 2,2,4,4,6,8,8-heptamethylnonane was added as the GC standard. The catalyst was introduced via syringe. Reactions were terminated and worked up in the same manner as for the ethylene polymerizations above.

Propylene Polymerization Procedures. Method 1 (−30 to 50 °C): A Schlenk, containing 100 mL of heptane, DMAO, and a magnetic stirrer under a nitrogen atmosphere, fitted with a rubber septum was purged under 1 bar of propylene overpressure for 5 min (to give 2 bar total propylene pressure). Al^{t}Bu$_3$ was added as a scavenger and the temperature of the vessel adjusted as required, allowing 20 min for the solvent to saturate with propylene. A toluene solution of precatalyst treated with 100 equiv of DMAO was introduced via syringe to initiate the polymerization. The reaction mixture was rapidly stirred throughout. Polymerizations were terminated by venting the overpressure followed by addition of 5 mL of 2 M $HCl_{(aq)}$. After warming to room temperature, a further 50 mL of 2 M $HCl_{(aq)}$ was added, and the layers were separated. The organic fraction was washed with 2 M $HCl_{(aq)}$ (50 mL) and water (50 mL), dried ($MgSO_4$), and filtered. The solvent was removed under vacuum and the polymer dried under high vacuum for 12 h.

Method 2 (−50 °C): The vessel was prepared as in method 1, except no solvent was added, and then placed in a cold bath at −50 °C. When 100 mL of propylene had condensed, the Schlenk was isolated from the propylene feed. A toluene solution of precatalyst treated with 100 equiv of DMAO was introduced via syringe to initiate the polymerization. The reaction mixture was rapidly stirred throughout. Polymerizations were terminated by addition of 5 mL of 2 M $HCl_{(aq)}$. The vessel was **SLOWLY** vented and warmed to room temperature. The polymer was isolated as for method 1.

Acknowledgment. BP Chemicals and, subsequently, Innovene and Ineos are thanked for financial support of this work.

Supporting Information Available: Crystallographic details, VT-NMR spectra, kinetic data, polymer NMRs, and GC results.

OM7008149